Real space origin of temperature crossovers in supercooled liquids

Ludovic Berthier[1,2] and Juan P. Garrahan[1]
[1]*Theoretical Physics, University of Oxford, 1 Keble Road, Oxford OX1 3NP, United Kingdom*
[2]*Laboratoire des Verres, Université Montpellier II, 34095 Montpellier, France*
(Received 18 June 2003; published 14 October 2003)

We show that the various crossovers between dynamical regimes observed in experiments and simulations of supercooled liquids can be explained in simple terms from the existence and statistical properties of dynamical heterogeneities. We confirm that dynamic heterogeneity is responsible for the slowing down of glass formers at temperatures well above the dynamic singularity T_c predicted by mode-coupling theory. Our results imply that activated processes govern the long-time dynamics even in the temperature regime where they are neglected by mode-coupling theory. We show that alternative interpretations based on topographic properties of the potential energy landscape are inefficient ways of describing simple physical features which are naturally accounted for within our approach. We show in particular that the reported links between mode coupling and landscape singularities do not exist.

DOI: 10.1103/PhysRevE.68.041201 PACS number(s): 47.10.+g, 64.70.Pf, 05.50.+q, 64.60.−i

I. INTRODUCTION

The aim of this paper is to critically reconsider the physical origin of the onset of dynamical arrest and the associated crossovers between distinct dynamical regimes displayed by liquids supercooled through their melting temperature towards the glass transition [1–4]. We do this by extending the real space theoretical framework based on dynamic facilitation of Refs. [5–8] to the moderately supercooled regime corresponding to the region where mode coupling theory (MCT) [9] supposedly applies, as reviewed in Refs. [10,11]. Our approach takes directly into account the spatial aspects of the dynamics, in particular those related to dynamic heterogeneity [12], in contrast with many other theories [3,4,9]. Our analysis shows that the onset of slowing down can be understood in a simple physical way in terms of the dynamical properties of effective excitations, or defects, as a progressive crossover from a regime of fast dynamics dense in defect clusters, to one of slow heterogeneous dynamics dominated by isolated localized defects. We demonstrate that this real space picture explains the observed crossover temperatures, challenges the idea that these crossovers are related to changes in the topography of the energy surface or to MCT singularities, and is able to account for the apparent correlations observed between ''landscape'' and dynamical properties.

The paper is organized as follows. In the rest of the introduction we review the MCT and energy landscape points of view, discuss their problems and limitations, and describe the alternative real space perspective we will pursue. In Sec. II we develop the physical picture of the onset of slowing down and dynamical crossovers which emerges from our theoretical approach. In Sec. III we discuss its quantitative consequences and compare them to published numerical results. In Sec. IV we show how our approach also enables to derive the observed properties of the potential energy landscape of supercooled liquids. Finally, in Sec. V we discuss our results and state our conclusions.

A. MCT/landscape scenario

It is often assumed that the initial slowing down of the dynamics of supercooled liquids can be rationalized by MCT [1–4,10,11]. Numerical simulations are now able to investigate the first five decades in time of this slowing down [11], so this is also the regime which has been studied in greatest microscopic detail. The degree of success of MCT is still a matter of debate. This is due to the fact that the central MCT prediction, a complete dynamical arrest at a temperature T_c where the α-relaxation time diverges as a power law, $\tau_\alpha(T) \sim (T-T_c)^{-\gamma}$, is actually never observed, but a power-law fit to the data apparently works on a restricted time window [10,11]. The appearance of new mechanisms for relaxation, often termed ''activated processes,'' but seldom described in any detail, is then invoked to explain the discrepancy between observations and MCT predictions. In fact, activated processes are actually quantitatively defined, within MCT, by deviations between data and predictions [11,13,14]. It is believed that activated processes become relevant close to the dynamical singularity T_c, their main effect being to prevent the predicted transition.

From T_c downwards it is assumed that the physics is dominated by activated processes, which determine also the canonical features of glass transition phenomena [15]: non-exponential relaxation, strong and fragile liquid behaviors, decoupling between transport coefficients, etc. It is sometimes said that the relevant physics for the glass transition sets in at T_c, and is therefore out of reach of numerical simulations [16]. Crossovers into the activated dynamics regime are also reported to occur at temperature T_x [17] or T_B [18], depending on which aspect of the physics is considered. It is believed that all these temperatures are close enough to be taken as equivalent, $T_c \approx T_x \approx T_B$ [19].

The above scenario is apparently corroborated by the study of the statistical properties of the potential energy landscape of model liquids [3,20–22]. From the properties of the landscape two temperatures seem to emerge, T_o and T_c [23]. The onset of slowing down of the dynamics takes place at T_o, and coincides with the temperature below which the average energy of inherent structures (IS), i.e., local minima of the potential energy [21], $e_{IS}(T)$, starts to decrease markedly, see Fig. 1. This has been interpreted as the sign that the landscape starts to ''influence'' the dynamical behavior [23]. At T_c, it is further argued, a second change in the landscape

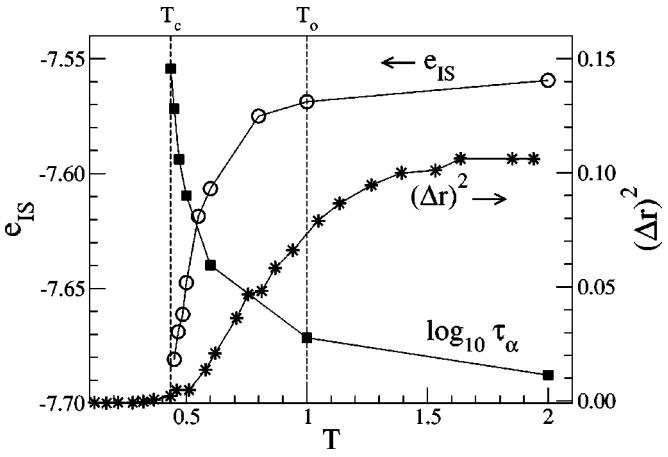

FIG. 1. Onset of slowing down in the binary Lennard-Jones mixture of Ref. [13]. Three quantities are reported as a function of temperature T. (i) The logarithm of the relaxation time, $\log_{10}\tau_\alpha$ (in arbitrary units extending over four decades in time); a MCT power-law divergence, with $T_c=0.435$, was used to fit this data in Ref. [13]. (ii) The energy of inherent structures, e_{IS}, taken from Ref. [43], which decreases markedly when the temperature decreases below $T_0=1.0$. (iii) The anharmonic part of Cartesian distance between configurations and their corresponding IS, $(\Delta r)^2 \equiv N^{-1}\Sigma_i(\mathbf{r}_i-\mathbf{r}_i^{(\mathrm{IS})})^2-aT$, which displays a qualitative change around T_c, taken from Ref. [23].

properties takes place, which is indicated by several observations [23–29]. For example, the mean-square displacement from an equilibrated configuration to its corresponding inherent structure, $N^{-1}\Sigma_i(\mathbf{r}_i-\mathbf{r}_i^{(\mathrm{IS})})^2$, is proportional to T below T_c, as expected from pure vibrations in quadratic wells, but the temperature dependence changes above T_c, revealing ''anharmonicities'' in the landscape [23,24], see Fig. 1.

Another indication of a topological change in the energy landscape was discussed in Ref. [30], in analogy with what happens in mean-field models [31,32]: the vanishing as T approaches T_c of the mean intensive number of negative directions (intensive index) of stationary points of the potential energy, $n_s(T)$. Numerical simulations [33–38] found that $n_s(T)$ decreases with decreasing T, and fits were performed to show that $n_s(T_c)=0$ [33–35]. The physical interpretation of this result is the apparent existence at T_c of a ''geometric transition'' between a ''saddle dominated regime'' above T_c and a ''minima dominated regime'' below T_c [39]. T_c would then really coincide with the appearance of activated processes, described in a topographic language as ''hopping'' between minima of the landscape. Analogous findings had been previously reported from instantaneous normal mode analysis of equilibrium configurations [40], also supporting a qualitative change in the landscape topology close to T_c [41,42].

Figure 1 summarizes this MCT/landscape scenario with published numerical data [13,23,43] obtained for the standard supercooled liquid model of Ref. [13].

B. Problems and contradictions

At first sight Fig. 1 appears as convincing evidence in favor of the MCT/landscape interpretation of the dynamics. On closer inspection, however, the above scenario is less robust. Several qualitative and quantitative observations do not fit into the picture presented above.

(i) Activated dynamics above T_c. The main idea behind the landscape approach [20] is that vibrations and structural relaxations take place on very different time scales, so that the system is ''trapped'' and vibrates in one minimum before ''hopping'' to another minimum. This is indeed observed using the mapping from trajectories to IS [21] in simulations of sufficiently small systems [44,45]. We have also discussed theoretically this issue in a recent work [6]. Given that numerical studies were performed much above T_c, a crucial conclusion of Refs. [6,44,45] is that ''activated dynamics'' is indeed present in this temperature regime.

(ii) Heterogeneous dynamics above T_c. It is now well documented that the dynamics of supercooled liquids, even above the mode-coupling temperature T_c, is heterogeneous in the sense that the local relaxation time has nontrivial spatial correlations [46]. This phenomenon is not very different from what happens experimentally close to the glass transition T_g [12]. Besides, the decoupling between transport coefficients, which is also interpreted in terms of dynamical heterogeneity [12,47], is observed in numerical simulations above T_c [13], although the effect is quantitatively less pronounced than in experiments near T_g [48].

(iii) Presence of saddles below T_c. Despite claims based on numerical results that T_c marks a real change in the topology of the landscape [33–35], there are strong indications that this is at best only a crossover [36,37], and at worst a biased interpretation of numerical data [38]. For instance, careful numerical studies have shown that the saddle index $n_s(T)$ remains positive even below T_c [36]. Moreover, Ref. [38] argues convincingly that the data for $n_s(T)$ can be described by an Arrhenius law, $n_s(T)\sim\exp(-E/T)$, with E an energy scale, which means that T_c does not mark any particular change in the saddle index.

C. Alternative: real space physics and coarse-grained models

The problems described above can be overcome through an alternative perspective on glass transition phenomena which puts the real space aspects of the dynamics at its core. This is the approach developed in Refs. [5–8]. Interestingly, several of its central concepts, such as the relevance to the dynamics of localized excitations [49,50] and the importance of effective kinetic constraints [51,52], have been present in the literature for many years. Moreover, one of the original key observations of dynamic heterogeneity in glass formers was made by Harrowell and co-workers [53] in the models of Ref. [52]. See Ref. [54] for an exhaustive review.

Our approach relies on only two basic observations.

(i) At low temperature mobility within a supercooled liquid is sparse and very few particles are mobile. This is somewhat equivalent to the statement that particles are ''caged'' for long period of times, as reflected by a plateau in the mean-square displacement of individual particles.

(ii) When a microscopic region of space is mobile it influences the dynamics of neighboring regions, enabling them to become mobile, and thus allowing mobility to propagate in the system. This is the concept of dynamic facilitation

[50,52]. The observation that very mobile particles in a supercooled liquid move along correlated ''strings'' [46] is a confirmation of this fundamental idea.

From these two concepts it is possible to build effective microscopic models for glass formers by means of a coarse-graining procedure. This procedure can be schematically described as follows [7]. Spatially, the particles are coarse grained over a length scale δx of the order of the static correlation length given by the pair correlation function. This removes any static correlations between coarse-grained regions of linear size δx. Cells are then identified according to their mobility by performing a coarse-graining on a microscopic time scale δt. In its simplest version cells are identified by a scalar ''mobility field,'' $n(\mathbf{r},t)=0,1$, the values 0/1 corresponding to an immobile/mobile cell at position $\mathbf{r}$ and time t. The next step is to replace continuous space by a lattice, $n(\mathbf{r},t)\rightarrow n_i(t)$. Mobile or excited cells carry a free energy cost, so when mobility is low it is reasonable to describe their static properties with a noninteracting Hamiltonian [52],

$$H=\sum_{i=1}^{N} n_i, \tag{1}$$

for a lattice of N sites. The link between mobility and potential energy [5] has also been observed in numerical simulations [46].

The coarse-graining procedure described above will generate local dynamical rules for the mobility field. The prominent feature of this dynamics will be dynamic facilitation, which in its simplest version states that a cell at site i is allowed to move only if it has an excited nearest neighbor [52],

$$n_i=0 \underset{\mathcal{C}_i(1-c)}{\overset{\mathcal{C}_i c}{\rightleftarrows}} n_i=1, \tag{2}$$

where $\mathcal{C}_i=1-\Pi_{\langle j,i\rangle}(1-n_j)$, and $\langle j,i\rangle$ indicates nearest neighbor, and c represents the average concentration of excited cells easily deduced from Eq. (1),

$$c(T)\equiv\langle n_i\rangle=(1+e^{1/T})^{-1}. \tag{3}$$

Explicit examples where dynamic facilitation is generated under coarse graining can be found in Ref. [55]. Clearly, different models are defined simply by changing the kinetic rules, e.g., the number or directionality of mobile neighbors required to move [54]. Also, a more complex mobility field may be required to account quantitatively for all glass transition features [7].

Crucially, we will show that the physical mechanisms which explain the onset of slowing down and crossovers between different dynamical regimes in supercooled liquids are generic to this class of models. This means that we can use the simplest of them, the Fredrickson-Andersen (FA) model defined by Eqs. (1) and (2) in one spatial dimension (hereafter 1D FA model) to make detailed predictions and calculations.

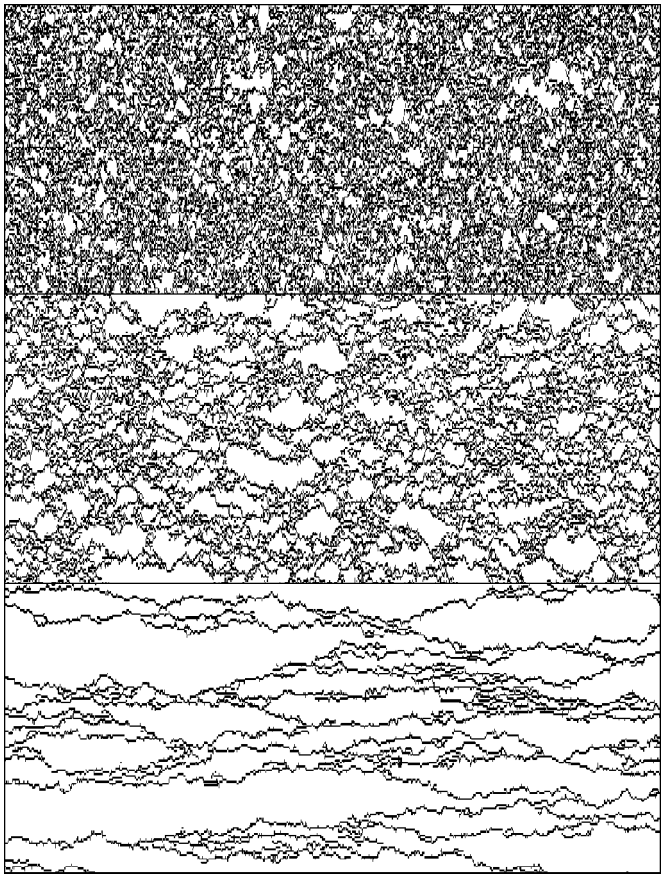

FIG. 2. Representative trajectories in the 1D FA model. The vertical axis is space, the horizontal one time. The three trajectories are for $L=150$ and $t=2000$. Excited cells (or defects) are black, unexcited ones white. The top frame is for $T=2.5$, in the high-temperature regime where almost no isolated defects are present. The middle frame is for $T=1.0$, the temperature regime where slow bubbles start to appear, seen here as large white domains. The bottom frame is for $T=0.5$, where almost all defects are isolated. For $T=0.5$, the mean relaxation time is ~ 120, the mean dynamic correlation length ~ 9, but it is clear that times and lengths are broadly distributed.

II. PHYSICAL PICTURE OF DYNAMIC CROSSOVERS

In order to understand the physics captured by the coarse-grained facilitated models defined above, it is useful to look at trajectories, that is, space-time representations of the dynamics [5]. We show in Fig. 2 three representative trajectories for the 1D FA model, where mobile cells (defects) are black, and immobile ones are white. From the trajectories, the principal observation is the appearance at low temperatures of nontrivial spatiotemporal correlations, seen as spatially and temporally extended domains of immobile cells delimited by isolated defects [5]. In 1D they look like ''bubbles'' [6], and trajectories are dense assemblies of these slow bubbles. This nanoscopic ordering in trajectory space is the cause of the phenomenon of dynamic heterogeneity observed experimentally and in simulations [5]. Dynamic heterogeneity is the central aspect of the physics of supercooled liquids: it is naturally captured by our approach.

The statistical mechanics of trajectories, rather than con-

figurations, determines the dynamical behavior. For example, due to the noninteracting Hamiltonian (1), static correlations are trivial. However, when trajectories are considered, it is clear that cells become dynamically correlated. In other words, these models naturally predict the existence of a dynamical correlation $\ell(T)$ which grows when the dynamics slows down. This statement can be quantified [5,8,56,57] by studying multipoint functions, for example, $C(|i-j|,t) = \langle P_i(t)P_j(t)\rangle - \langle P_i(t)\rangle\langle P_j(t)\rangle$, where $P_i(t)$ is a dynamical correlator at site i (below we will consider the persistence of site i). The spatial decay of a function like $C(|i-j|,t)$ defines unambiguously the dynamical correlation length $\ell(T)$, as already discussed theoretically [5,8,56] and measured in numerical simulations [46,56–59]. Furthermore, the joint distributions of time and length scales give rise to the canonical features of glass formers, such as stretched relaxation, decoupling between transport coefficients, and (kinetic and thermodynamic) strong and fragile behaviors [5–7].

Let us take a closer look at the temperature evolution of the trajectories in Fig. 2. Starting from the very low temperatures where trajectories consist of a mixture of slow bubbles, the dynamics can be understood in terms of the opening and closing of bubbles, that is, the branching of an excitation line or the coalescence of two. As shown in Ref. [6], these events are the ''hopping between minima'' described in Ref. [20]. Therefore, we have a clear understanding of ''activated processes'' and of their statistical properties [6].

As temperature is increased, more and more defects are present. This has several consequences. First, the typical spatial and temporal extension of bubbles reduces, that is, the system becomes faster and less heterogeneous. Second, clusters of defects become more common. These objects are important because their dynamics is completely different from that of isolated defects. In a cluster, defects do not have to diffuse and create or annihilate other defects but can instantaneously relax in a much faster process. At high temperature, the dynamics is fast because almost no bubbles are present, and the dynamics is governed by clusters of defects. Interestingly, at some intermediate temperature (middle frame in Fig. 2) a coexistence between clusters and isolated defects is observed, so that the dynamics has a ''mixed'' character.

Clusters of defects disappear much faster with decreasing temperature than the overall concentration of defects. The probability to have a cluster of k defects is indeed $p(k) \propto c^k$, so that at low T we have $p(1) \gg p(2) \gg \cdots$.

The coexistence of fast and slow processes with different temperature behavior has a direct influence on the distribution of local relaxation times, which we present in Fig. 3 for various temperatures. At high temperature, $T \gg 1.0$, where fast processes are dominant, the distribution is exponential, with a mean which depends weakly on temperature (below we discuss in detail its temperature dependence). Around $T = 1.0$, a shoulder develops in the large time tail of the distribution, corresponding to the appearance of the bubbles in the trajectories of Fig. 2. This marks the increasing relevance of slow processes and the growth of the dynamic correlation length beyond the microscopic high-temperature value. This

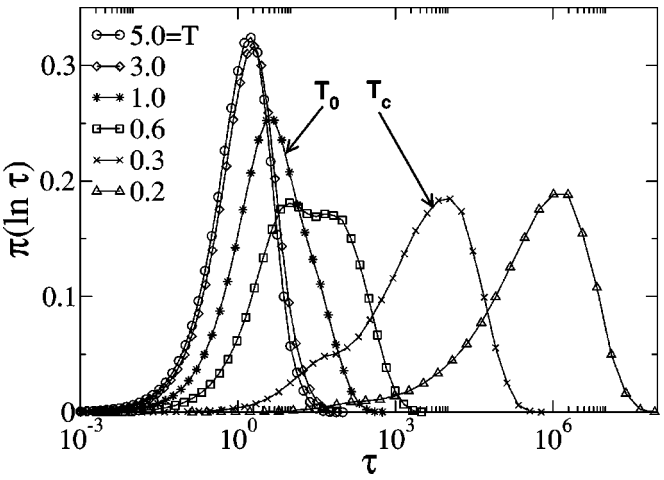

FIG. 3. Distribution of the logarithm of the persistence time of individual cells, $\pi(\ln\tau)$ for various temperatures. $T_o = 1.0$ marks the appearance of a shoulder in the high-temperature distribution. For $T_c < T = 0.6 < T_o$, two ''processes'' coexist. Fast processes disappear close to $T_c = 0.3$.

temperature corresponds therefore to the onset temperature $T_o = 1.0$.

Decreasing further the temperature, we clearly see a regime of mixed dynamics. At $T = 0.6$, for instance, there are two peaks in the distribution, reflecting the coexistence of clusters and isolated defects. At this temperature, the time scale has already increased by several orders of magnitude, and the dynamic correlation length is about $\ell(T=0.6) \approx c^{-1}(T=0.6) \approx 6$.

Finally, further decrease in temperature makes clusters of defects very rare and we are left only with the contribution of isolated defects. This low-temperature distribution is the one discussed in Refs. [5,6], which in turn implies the stretched exponential decay of dynamical correlators. The contribution of clusters becomes negligible beyond a second crossover temperature, here $T_c = 0.3$. While this crossover temperature is not linked in any way to the mode-coupling singularity T_c, this choice of notation will become clear shortly.

From these distributions, it is possible to propose an empirical but quantitative determination of T_o and T_c. At each temperature T, the distribution is composed of fast processes $\tau < \tau_\star(T)$, and slow processes $\tau > \tau_\star(T)$, where $\tau^\star(T)$ can be defined, e.g., as in Ref. [60]. Requiring that slow processes are a significant fraction (say 90%) of the distribution leads to the definition of T_c,

$$\int_{\tau_\star(T_c)}^{\infty} d\tau'\, \pi(\tau') = 0.9, \tag{4}$$

where in an abuse of notation we also call $\pi(\tau)$ the distribution of persistence times. Requiring that slow processes, while not dominant in number, still contribute to a significant fraction of the mean relaxation time (say again 90%) leads to the definition of T_o,

$$\int_{\tau_\star(T_o)}^{\infty} d\tau'\, \pi(\tau')\tau' = 0.9\ \langle\tau\rangle. \tag{5}$$

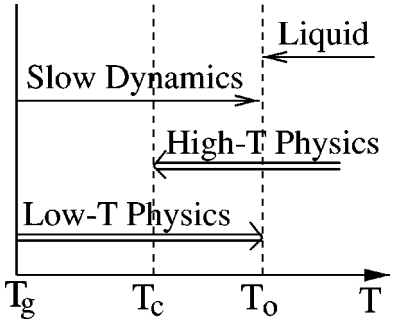

FIG. 4. Temperature regimes emerging from the discussion of Sec. II. T_0 marks the onset of slow dynamics, the appearance of the isolated defects (bubbles, activated processes), and the growth of a dynamic correlation length. At T_c, traces of the high-T physics (clusters) become negligible in the distributions of relaxation times. The crossover region $T_c<T<T_o$ has therefore a mixed character.

In Fig. 4, we summarize the physical picture that emerges from the considerations of this section. From the distributions of Fig. 3, we recognize that the dynamics becomes slow when the temperature is decreased below the onset temperature T_o. This distinguishes the trivial liquid and the slow glassy regimes. From the trajectories of Fig. 2, we were also able to distinguish between fast, nonactivated processes (clusters), and slow, activated processes (isolated defects, bubbles). The former, typical of the liquid high-T physics, become negligible below T_c, while the latter, typical of the low-T physics, appear at the onset temperature T_o. As a consequence, the crossover region $T_c<T<T_o$ contains traces of both high-T and low-T physics, as observed in the time distributions of Fig. 3.

III. QUANTITATIVE CONSEQUENCES

The physical picture we have presented for the onset of slowing down, based on the increasing relevance of a dynamically heterogeneous evolution of the system, leads to quantitative predictions which are in good agreement with previous numerical and experimental studies, as we discuss in this section.

A. Dynamical correlators

The basic dynamical quantities recorded in experiments and simulations of supercooled liquids are spatially averaged two-time functions. Simulations usually focus on the time domain and typically consider density-density correlation functions, while experimental results are often expressed in the frequency domain, measuring for instance dielectric susceptibilities. We will only consider systems in equilibrium so that the information content of both kinds of measurements is equivalent.

From the distributions of times, Fig. 3, it is easy to derive dynamical correlators for the 1D FA model considered here. The spatially averaged persistence function reads

$$P(t)=\int_t^\infty d\tau'\,\pi(\tau'). \tag{6}$$

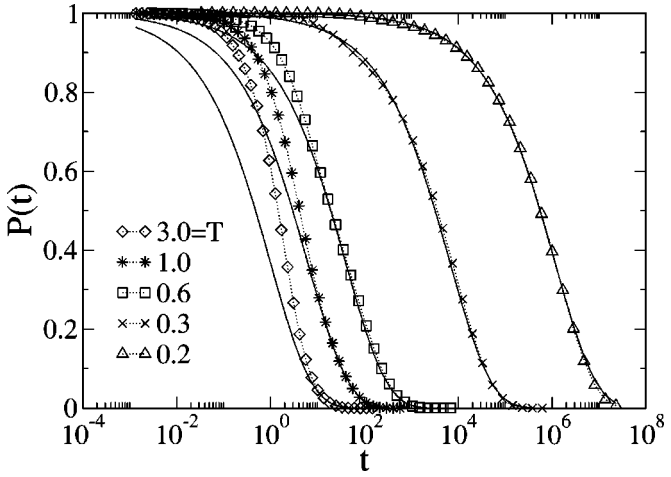

FIG. 5. Persistence functions in the 1D FA model for the same set of temperatures as in Fig. 3. Symbols are numerical data and full lines are fits to the stretched exponential form expected theoretically for low temperatures, $P(t)=\exp\{-[t/\tau(T)]^\beta\}$, with $\beta=1/2$.

The behavior of $P(t)$ as a function of time for various temperatures is shown in Fig. 5. At very low temperatures, the persistence function is known exactly due to the diffusion properties of isolated defects, and one gets

$$P(t)=\exp\left[-\left(\frac{t}{\tau(T)}\right)^\beta\right], \tag{7}$$

where $\tau(T)$ is the relaxation time discussed in the following section. For the 1D FA model, $\beta=1/2$, but the stretching exponent might be temperature dependent in more elaborated (fragile) models [6,54], as is indeed observed in experiments [1,2].

We see from Fig. 5 that for $T=0.2$ and 0.3 $P(t)$ is well approximated by Eq. (7) on the whole time window. For higher temperatures, $T>T_c=0.3$, the mixed character of the correlators is evident from the fact that Eq. (7) only describes the long time behavior of the correlator, as expected. In this temperature regime, short times are best described by a simple exponential. In the high-temperature regime, $T>T_o=1.0$, relaxation is just exponential for all times. We conclude that the appearance of isolated defects at T_o is reflected in the long-time behavior of dynamical correlators. In the crossover region, $T_c<T<T_o$, more and more of the decorrelation is due to isolated defects when T decreases. Below T_c the entire decorrelation is due to these slow processes.

A confirmation of the progressive domination of slow over fast processes described above can be found in the numerical results of Ref. [26]. The similarity of Fig. 4 of Ref. [26] and our Fig. 5 is in fact quite striking. In particular, Ref. [26] calculated density-density correlations from both real configurations and their corresponding IS in a binary Lennard-Jones mixture. The latter, where thermal energies were removed in the quenching procedure, are the ones which have to be compared with Fig. 5, since fast vibrations are also removed in our coarse-grained approach.

An important conclusion is that the long-time decay of dynamical correlators, sometimes referred to as the

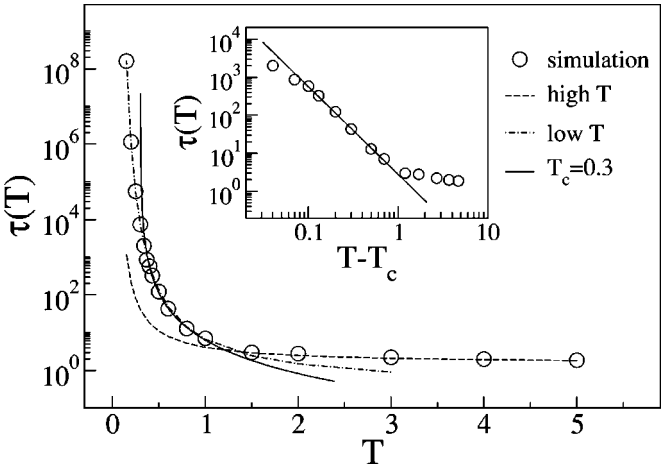

FIG. 6. Temperature dependence of the relaxation time in the 1D FA model, $\tau(T)$. Open circles correspond to numerical data. Three fits are presented. The dashed line is the simple mean-field Hartree-like approximation, $\tau_{\mathrm{MF}} \sim \exp(1/T)$. The dotted-dashed line is the low-T exact behavior, $\tau_{\mathrm{ex}} \sim \exp(3/T)$. The full line is a power-law MCT-like fit, $\tau_{\mathrm{MCT}} \sim (T-T_c)^{-\gamma}$ with $\gamma = 2.3$ and $T_c = 0.3$. The inset shows that the apparent power-law behavior is acceptable in a range of three decades in times. The main figure shows that low-T and high-T fits account for the whole temperature range.

α relaxation, is due to the presence of isolated defects and therefore of heterogeneous dynamics, even in the $T > T_c$ regime. This means that activated dynamics, in the language of MCT, or hopping events in topographic terms, are responsible for the α relaxation, even at temperatures well above T_c. This conclusion is unavoidable in view of the numerical data of Refs. [26,44,45].

B. Relaxation time

The next natural quantity to consider, the relaxation time $\tau(T)$, is readily obtained from the dynamical correlators discussed in the preceding subsection. From the discussion of Sec. II, we expect a crossover from high-T to low-T at the onset temperature T_o; see Eq. (5). Our results for the 1D FA model are presented in Fig. 6, where $\tau(T)$ is defined as the time where the persistence function has decayed to the value $1/e$.

The simplest mean-field approximation to the dynamics of the FA model consists in a Hartree-like decoupling of spatial correlations, $\langle n_i n_j \rangle \to n_i \langle n_j \rangle$, in the dynamical equation for n_i. This amounts to replacing the actual neighborhood of site i by an average neighborhood, and spins are always facilitated with an average rate equal to c. This gives a mean-field estimate of the relaxation time [61],

$$\tau_{\mathrm{MF}}(T) \approx c^{-1} \sim \exp\left(\frac{1}{T}\right). \tag{8}$$

Figure 6 shows that this simple approximation accounts for the dependence of the relaxation time at high-temperatures, $T \geqslant T_o$.

The exact result for the relaxation time of the 1D FA model is obtained by realizing that isolated defects undergo diffusion with a temperature dependent diffusion constant, $D(T) \approx c \sim \exp(-1/T)$. The system relaxes when defects have diffused over a distance given by the mean separation between defects, c^{-1}, so that

$$\tau_{\mathrm{ex}}(T) \approx D^{-1} c^{-2} \sim \exp\left(\frac{3}{T}\right). \tag{9}$$

This mechanism relies on the notion of dynamic facilitation which implies that local fluctuations of the mobility determine the dynamics, and is essentially beyond the reach of any mean-field type of approximation [53]. We see from Fig. 6 that Eq. (9) accounts for the behavior at low-temperatures, $T \leqslant T_o$. Figure 6 also presents a fit to the data with an MCT power-law form for the relaxation time [9],

$$\tau_{\mathrm{MCT}}(T) \approx (T - T_c)^{-\gamma}, \tag{10}$$

similar to the one obtained in Ref. [52] for the two-spin facilitated, two-dimensional version of the FA model.

From Fig. 6, we draw the following conclusions. The behavior of the relaxation time changes from the high-T to low-T behavior close to the onset temperature T_o. The combination of simple mean field at high T with the exact form at low T allows to describe the temperature dependence of the relaxation time over the whole temperature range. However, given that $\tau(T)$ smoothly interpolates between these two different functional forms, the MCT power-law form, Eq. (10), appears to work reasonably well in a time window of about three decades (see inset in Fig. 6). This range of apparent power-law behavior is in fact larger than the corresponding one in the canonical binary Lennard-Jones mixture of Ref. [13], where extensive tests of MCT have been performed. Remarkably, we also find that the T_c extracted from the power-law fit to the relaxation time coincides well with the temperature where fast processes cease to contribute in a significant manner to the distribution of relaxation times, Fig. 3. This explains our choice of notation for the lower crossover temperature T_c.

Following the standard MCT reading of the data [10,11,13], we would erroneously conclude that activated processes only appear close to $T_c = 0.3$, since these processes are often tautologically defined by the breakdown of the power-law behavior of the relaxation time [11]. Figures 3, 5, and 6 prove instead that activated dynamics starts to be relevant at T_o, much above T_c, dominating the α relaxation of the correlators, and hence the relaxation time of the system. The results of this section considerably weaken the possibility of the existence of a temperature regime in supercooled liquids where the relaxation time is correctly described by a power-law behavior. It follows that the standard determination of the location of the MCT "singularity" T_c in experiments and simulations is physically unjustified [62,63]. In fact, the issue of the location of T_c has been recently addressed in Ref. [64], where it was found that for a variety of systems, the temperature T_c obtained from the actual MCT equations systematically coincides with the onset temperature T_o discussed above.

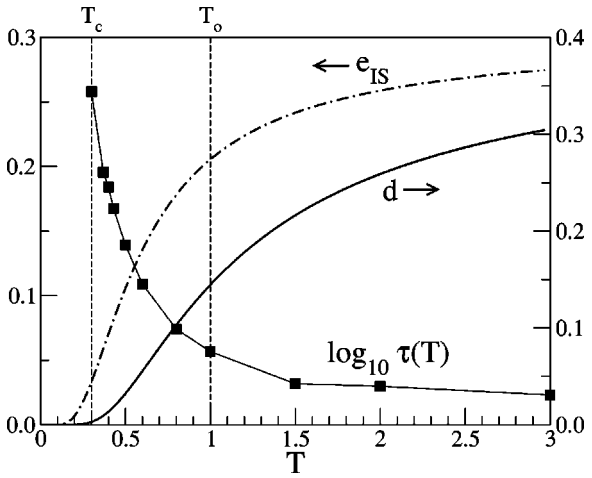

FIG. 7. Onset of the slowing down in the 1D FA model. We show three quantities as a function of temperature T. (i) Logarithm of the relaxation time, $\log_{10}\tau$, see Fig. 6. (ii) Energy of IS, e_{IS}, which displays a qualitative change around $T_o=1.0$. (iii) Concentration d of cells moved in the descent from an equilibrium configuration to its IS, which displays a qualitative change around $T_c=0.3$. This figure should be compared with Fig. 1.

C. Crossover temperatures

Let us now consider the quantities shown in Fig. 1 as evidence in favor of the MCT/landscape picture in Lennard-Jones mixtures, from the perspective of dynamically facilitated models. In Fig. 7 we show for the 1D FA model a plot analogous to Fig. 1.

The first quantity presented in Fig. 7 is the logarithm of the relaxation time, $\log_{10}\tau(T)$, as a function of temperature, which we discussed in detail in the preceding subsection.

The second quantity shown in Fig. 7 is the average energy of inherent structures, e_{IS}. For the 1D FA model it can be computed analytically by solving the zero-temperature dynamics of the model [65],

$$e_{IS}(T)=c\ \ e^{-c}, \tag{11}$$

where the concentration of defects, c, is defined in Eq. (3). At high-temperature e_{IS} changes very slowly. When T is reduced below T_o the concentration of defects starts to decrease markedly, and e_{IS} follows the same trend, as can be seen in Fig. 7. This change in behavior at the onset temperature T_o is due to the appearance of isolated defects, and therefore of a heterogeneous dynamics, and not to any special change of the potential energy surface. This is a very different interpretation of the physics from that of Ref. [23].

The third quantity shown in Fig. 7 is analogous to the distance between a configuration and its nearest IS (see Fig. 1). In the lattice models we are considering the natural quantity to compute is the concentration of sites which change during the descent towards the inherent structure, $d(T)$. Since only excited sites can change during this procedure, we get

$$d(T)=c-e_{IS}=c(1-e^{-c}). \tag{12}$$

Clearly, at low temperature $d\approx c^2\sim\exp(-2/T)$. This behavior is physically natural. Contributions to $d(T)$ come from clusters of defects, which are the only objects that can relax during the descent to an IS. Since the probability for a cluster of k defects, $p(k)$, goes as $p(k)\approx c^k$, the main nontrivial contribution to $d(T)$ at low T comes from the smallest clusters, $k=2$. These relax only one defect in the descent, so that $d\approx p(2)\approx c^2$. Moreover, our defect interpretation is consistent with real space observations in simulations of silica [27], where it was found that during the descent to the IS the major contribution to the distance comes from annihilation of localized topological defects of the amorphous structure.

The similarity of Fig. 7 to Fig. 1 is striking. The emerging physical picture, is however, completely different from the one of the MCT/landscape scenario. For example, while it may appear from the behavior of $d(t)$ above T_c that this quantity extrapolates to zero when $T\to T_c$ (see Fig. 7), the exact temperature dependence of $d(T)$ is purely Arrhenius. This means that T_c has no particular importance [T_c would not look special in a plot of $d(T)$ versus $1/T$]. Even if one accepts T_c as delimiting two regimes with high and low concentrations of clusters of excitations, this apparent crossover is completely irrelevant as far as the long-time dynamics is concerned. These observations suggest that the crossover at T_c from ''landscape influenced'' to ''landscape dominated'' of Ref. [23] is not physically significant for the α relaxation.

IV. INTERPRETATION OF "LANDSCAPE" PROPERTIES

In recent years, the potential energy landscape of supercooled liquids has become an object of study *per se* [3]. In Ref. [6], we have developed the idea that the main motivation behind these works was the observation of the separation between fast vibrations and slow hopping processes if sufficiently small systems are considered. This apparently harmless statement on the system size, we argued in Ref. [6], results in fact from the central feature of the dynamics of supercooled liquids: ''sufficiently small'' really means ''if the system size is of the order of the dynamical correlation length $\ell(T)$'' [6,25]. However, in a purely topographic description of the physics based on the statistical properties of minima, the relevance of the dynamical correlation length is not obvious [66]. In that sense, a topographic description of the glass transition misses a central aspect of the physics.

We shall show below that using the very simple spatial approach described in previous sections, we can trivially derive the statistical properties of the landscape reported in recent years. This successful confrontation to such an amount of apparently nontrivial and detailed numerical results is again a strong indication of the validity of our approach.

A. Real space description of "minima" and "saddles"

Reference [6] described in detail the connection between the nanoscopic ordering in the trajectories of dynamically facilitated models and the dynamics between IS, ''metabasins,'' or ''traps'' observed in numerical simulations or experiments of supercooled liquids. This same approach can be

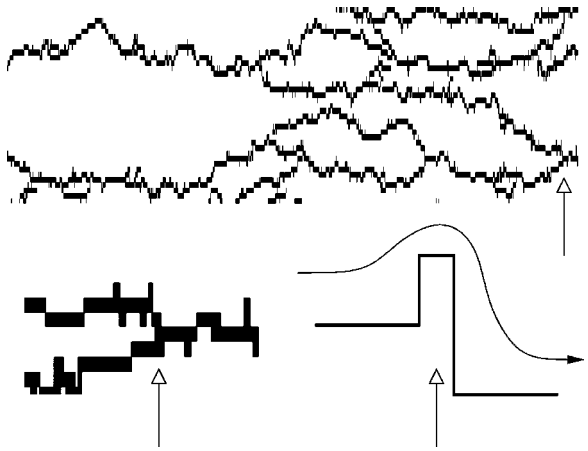

FIG. 8. Top: zoom on the low-T trajectory of Fig. 2. The vertical arrow indicates the closing of a bubble. Bottom left: expanded view of this event, showing two excitation lines meeting and coalescing. A cluster of three spins is needed for this process to occur. Bottom right: corresponding ''reaction path.'' Before the event there are two isolated defects (energy $=2$), a cluster of three defects (energy $=3$) during the event, and one isolated defect after (energy $=1$).

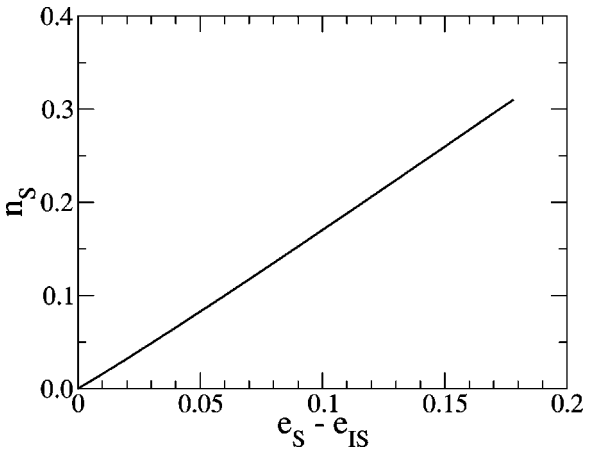

FIG. 9. Saddle index versus energy difference between saddle and minima computed analytically for the 1D FA model for $T \in [0,\infty)$ and $p_s=1/2$. The obtained linear behavior is a natural consequence of (i) dynamic facilitation, (ii) localized defects, and (iii) dynamic heterogeneity.

extended to account for the properties of ''saddles,'' i.e., configurations related to transitions between IS.

Figure 8 zooms on the lowest-temperature trajectory of Fig. 2. The top panel of Fig. 8 shows diffusion of isolated defects. It also shows coalescence and branching events, i.e., closing and opening of bubbles. These two kinds of processes correspond to ''hopping'' events between dynamical ''traps'' [6]. Let us consider in detail one of these events, for example, the coalescence process enlarged in the bottom left panel of Fig. 8. Isolated defects diffuse by first facilitating one of their neighbors, for instance,

$$10 \rightarrow 11 \rightarrow 01. \tag{13}$$

For two defects to coalesce the minimum number of excitations that have to be present when they merge is three,

$$101 \rightarrow 111 \rightarrow 011 \rightarrow 010. \tag{14}$$

In this sequence, the total number of defects is 2 at the beginning, 3 at the transition, and 1 at the end. This process is schematically described in the bottom right panel of Fig. 8.

In topographic terms, an isolated defect corresponds to a local minimum of the energy, since such a configuration can only evolve by an energy increase, as in Eq. (13). On the other hand, a cluster of three excitations corresponds locally to a saddle point, since it is the transition configuration between two minima, as in Eq. (14) and Fig. 8. Larger clusters thus correspond to higher order saddles, since the larger the cluster the larger the number of possible moves into minima. The case $k=2$ is particular: it is not a minimum since it can relax one defect to decrease its energy, but it is not a saddle either since it does not correspond to a hopping event like that of Fig. 8. Clusters with $k=2$ are just ordinary points (i.e., not stationary points) of the landscape. The previous discussion generalizes in a natural way to the whole class of dynamic facilitated systems.

B. Absence of "geometric transition"

The above identification between the relevant dynamical objects, isolated defects and clusters of defects, and ''landscape properties'' allows one to compute quantities such as the mean saddle index, $n_s(T)$, and the corresponding mean energy of stationary points, $e_s(T)$.

The quantities n_s and e_s were estimated numerically in simulations of supercooled liquids [33,34]. It was found that both functions decrease when T decreases, and extrapolations were performed that indicated $n_s(T_c)=0$. Also, plotting the dependence of n_s on e_s-e_{IS} parametrized by the temperature, a simple linear relation was obtained, $n_s \propto (e_s-e_{IS})$ [33–35].

In the case of the 1D FA model, it is very simple to devise a procedure to go from an equilibrium configuration to the ''nearest'' stationary point. Isolated defects and clusters of defects with $k \geqslant 3$ are locally such points, so we only have to deal with $k=2$ clusters. From these we can either reach a ''minimum'' $k=1$ or a saddle with $k=3$. We, respectively, assign the probabilities p_s and $(1-p_s)$ to these two possibilities. We then have

$$n_s(T)=\sum_{k=1}^{\infty} p(k) n_s(k) \tag{15}$$

and

$$e_s(T)=\sum_{k=1}^{\infty} p(k) e_s(k), \tag{16}$$

where $p(k)=(1-c)^2 c^k$ is the probability to have a cluster of size k. From the discussion above we know that $n_s(1)=0$, $e_s(1)=1$, $n_s(2)=(1-p_s)$, $e_s(2)=p_s+3(1-p_s)$, $n_s(k \geqslant 3)=e_s(k \geqslant 3)=k$. Putting all together we obtain

$$n_s(T)=3c^2\left[(1-p_s)(1-c)^2+c\left(1-\frac{2}{3}c\right)\right] \tag{17}$$

and

$$e_s(T) = c + (1-2p_s)c^2(1-c)^2. \tag{18}$$

At low T both quantities scale as $n_s \sim c^2$ and $e_s \sim c$. Three important conclusions can be drawn.

(i) It is obvious from Eq. (17) that $n_s(T) > 0$ for $T > 0$. This means that there is no ''geometric transition'' to a regime with vanishing saddle index.

(ii) The saddle index has a temperature dependence which follows closely that of the distance $d(T)$ discussed in the preceding subsection. This is expected because they both receive their principal contribution, at low T, from clusters with $k=2$. In other words, the main objects for the low-temperature dynamics, the isolated defects, do not contribute to these quantities. Therefore, as for the distance $d(T)$ in Fig. 7, the rapid decrease of $n_s(T)$ when the temperature decreases can easily be confused with a vanishing of the saddle index close to T_c.

(iii) The linear relation between n_s and $e_s - e_{IS}$ becomes exact at low-temperatures, see Eqs. (11), (17), and (18). Again, the difference between e_s and e_{IS} comes from the clusters of defects which are relaxed during the descent to the inherent structure. In Fig. 9, we show the behavior of n_s versus $e_s - e_{IS}$ for the entire range $T \in [0,\infty)$. Note that in Ref. [33] a linear behavior between n_s and e_s was also reported. This is true at relatively high temperature, given that above T_o the energy of inherent structure is almost constant while n_s and e_s change with temperature in the same way.

These results are valid beyond the FA model which we have used to illustrate them. The inexistence of the geometric transition where the saddle index vanishes follows from the observation that the low-temperature behavior of n_s is given by the smallest cluster of defects necessary to make a transition, in the sense described in the preceding section. Since these objects are spatially localized, their energy cost is $O(1)$, and they exist with non zero probability at finite temperature $T > 0$. This argument is close in spirit to Stillinger's argument for the inexistence of an entropy crisis at the Kauzmann temperature involving point defects [67]. Moreover, as discussed in the Introduction, careful numerical simulations both confirm that $n_s(T < T_c) > 0$ [36,37], and report an Arrhenius behavior $n_s(T)$ [38], in agreement with our results.

The relation between saddle index and energy,

$$n_s \propto (e_s - e_{IS}), \tag{19}$$

which was first observed numerically [34,33,35], is also a general result for dynamically facilitated systems. This relation contains two different pieces of information. First, it shows that the intensive saddle index is a number of $O(1)$. This is again a trivial consequence of the existence of the dynamical correlation length $\ell(T)$, so that a large sample can, in fact, be thought of an assembly of independent subsystems of linear size $\ell(T)$ [6]. Second, and more interesting, is a connection between energy and saddle index, presented as a ''general feature of the potential energy landscape of supercooled liquids'' [35], for which no theoretical explanation was, however, available. This feature is, in fact, almost a tautology in the context of facilitated models: the more defects are present, the more available directions to move, the higher the energy above that of the IS. The fact that relation (19) holds in different model liquids is another confirmation that dynamical facilitation is a key generic feature of the dynamics of supercooled liquids.

C. Thermodynamics and "anharmonicities"

Another common procedure of the landscape approach is to decompose configurations into vibrational and configurational components. Stillinger and Weber [22] suggested to perform this decomposition at the level of the partition function,

$$Z(T) \approx \sum_{E_{IS}} \Omega(E_{IS}) \exp\left(-\frac{E_{IS} + F(T;E_{IS})}{T} \right), \tag{20}$$

where the sum is over energies of IS, E_{IS}, their number is indicated by $\Omega(E_{IS})$, and $F(T,E_{IS})$ is the ''basin free energy'' which takes into account fluctuations within an IS due to vibrations and possible ''anharmonicities'' (i.e., all the rest).

It is instructive to consider the calculation of the partition function in the case of the 1D FA model using the Stillinger and Weber decomposition. The thermodynamics of the FA model is that of a noninteracting gas of binary excitations. This simple thermodynamics, however, can be obtained with any dynamics obeying detailed balance with respect to Hamiltonian (1), the actual FA dynamics defined by Eq. (2) being just one possibility. In this sense, the Stillinger and Weber prescription for thermodynamics is an approximation for the way a thermodynamic quantity would be calculated using a particular choice of dynamics to sample the configuration space. Inherent structures, basin free energies, etc., have no thermodynamic meaning, they only have a dynamical meaning associated with a particular choice of dynamics.

For the 1D FA model we can evaluate the Stillinger and Weber partition function exactly. We have

$$Z_N(T) = \sum_{E_{IS}=0}^{N/2} \frac{(N-E_{IS})!}{E_{IS}!(N-2E_{IS})!} \exp\left(-\frac{1}{T}[E_{IS} + F_{\mathrm{anh}}(T;E_{IS})] \right). \tag{21}$$

The first factor counts the number of configurations of energy E_{IS} with only isolated defects in a system of N sites. Due to the coarse-grained nature of facilitated models the only contribution to the basin free energy comes from anharmonicities.

Performing the sum in Eq. (21) without the anharmonic contribution gives

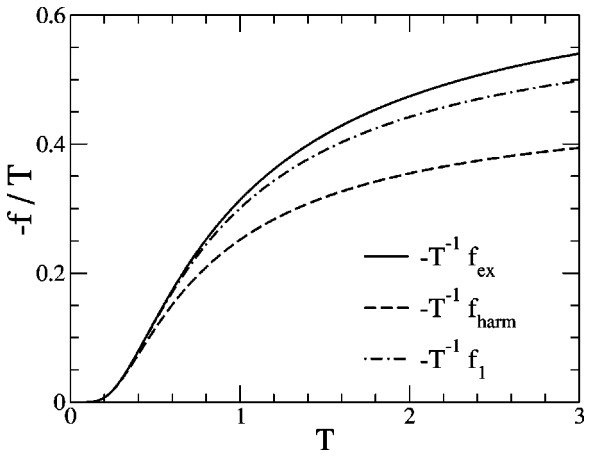

FIG. 10. Comparison of the various expressions for the free energy (divided for convenience by $-T$) in the 1D FA model: $f_{\rm ex}$ is the exact free energy (24); $f_{\rm harm}$ is the purely harmonic evaluation (23) which is a good approximation below $T_c=0.3$, and f_1 is the result obtained with expression (26) for anharmonicities which is good up to $T_o=1.0$.

$$Z_N^{\rm harm}(T)=\exp\left(-\frac{N}{2T}\right)U_N\left[-\frac{i}{2}\exp\left(\frac{1}{2T}\right)\right], \qquad (22)$$

where $U_N(x)$ is the Nth Chebyshev polynomial of second kind. In the thermodynamic limit the above expression simplifies to give the free energy in the ''harmonic'' approximation,

$$f_{\rm harm}(T)=\lim_{N\to\infty}-\frac{T}{N}\ln Z_N(T)$$
$$=T\ln 2-T\ \ln(1+\sqrt{1+4\ \ e^{-1/T}}). \qquad (23)$$

In Fig. 10, we compare approximation (23) to the exact expression for the free energy,

$$f_{\rm ex}(T)=-T\ln(1+e^{-1/T}). \qquad (24)$$

As observed numerically in supercooled liquids [3], both thermodynamic evaluations, Eqs. (23) and (24), apparently coincide below T_c when anharmonicities become negligible. From the previous sections we know that anharmonicities are just a consequence of the existence of clusters of defects. At low-temperature the difference between Eqs. (23) and (24) is therefore proportional to c^2, reflecting the fact that: (i) anharmonicities do not disappear below T_c, which again is no particular temperature in this context; (ii) anharmonicities are due to clusters of defects, $k=2$ being the leading term at low temperatures.

In the particular case of the FA model we can formulate an exact expression for the anharmonic free energy $F_{\rm anh}$. It is easy to check that the choice

$$F_{\rm anh}(T;E_{IS})=E_{IS}(T)\ \ f_{\rm ex}(T) \qquad (25)$$

in Eq. (21) yields the exact expression for the free energy in the thermodynamic limit. This exact expression for the anharmonic part of the free energy is simple to understand. In an IS all defects are isolated. The contribution of clusters of defects is obtained from the probability that an isolated defect in the IS was a cluster in the original configuration, which is given by Eq. (25).

Interestingly, a numerical procedure to evaluate the anharmonic contributions can be proposed. First, the harmonic expression (23) is evaluated. Then, the approximate expression

$$F_{\rm anh}(T;E_{IS})\sim E_{IS}(T)f_{\rm harm}(T) \qquad (26)$$

can be used as an educated guess for the anharmonic contributions. This gives in turn a first order free energy $f_1(T)$. The improvement on the harmonic evaluation can be judged in Fig. 10, where we see that $f_1(T)$ coincides with the exact free energy up to $T\sim T_o$. This evaluation can then be improved iteratively using $F_{\rm anh}(T;E_{IS})\sim E_{IS}(T)f_1(T)$ to get $f_2(T)$, and so on. It is easy to show that, in our particular case, $\lim_{n\to\infty}f_n(T)=f_{\rm ex}(T)$.

Although these results could lead to an improvement on present evaluations of anharmonic contributions in studies of the thermodynamics of supercooled liquids, they also show that topographic concepts are very far from the physical objects they pretend to describe.

D. Failure of the Adams-Gibbs relation

We end this section with a remark on the Adam-Gibbs relation, which is an attempt to connect dynamical properties to thermodynamic ones. The Adam-Gibbs formula relates the relaxation time of a glass former τ_α to the configurational entropy S_c [which would correspond to $S_c=\langle\ln\Omega(E_{IS})\rangle$ in the IS formalism]: $\tau_\alpha\propto\exp[1/(TS_c)]$. Apparently, this relation has been seen to hold both in numerical simulations and in experiments of various systems [3]. A careful look at the published data reveals, however, that the correlation between relaxation time and entropy does not quantitatively satisfy the Adams-Gibbs relation. This important observation is often not clearly stated [3].

Our analysis shows indeed that thermodynamic properties do not fully determine dynamical behaviors. Clearly, almost by definition, τ_α increases and S_c decreases as temperature is lowered, but that is where the connection ends. It is easy to check that the Adam-Gibbs formula fails completely when applied to dynamic facilitated systems. We find instead that time scales are broadly distributed, the distribution of times being the result of an integral over a distribution of length scales, $\rho(\ell)$, imposed by thermodynamic equilibrium, Eq. (1). Crucially, however, dynamics also enters the integral in the form of the conditional probability of time and length, $\rho(t|\ell)$, which can be described, in a topographic language as containing information on the relevant ''barriers,'' which have *a priori* no obvious link with the statistics of minima. As a consequence, thermodynamics alone cannot be used to predict the dynamical behavior. Again, we find in the literature an excellent numerical confirmation of this statement. In Refs. [38,60], using a purely topographic description of a supercooled liquid, it was shown that the diffusion constant

could be computed by a combination of thermodynamic *and* dynamical quantities, well in line with the above discussion.

V. CONCLUSIONS

In this paper, we have developed a spatial description of the physics of the progressive slowing down of supercooled liquids. The only ingredients in our method have been the notions of localized mobility excitations and facilitated dynamics [5–8]. Our results were illustrated explicitly for the simplest case of the 1D FA model, but are generic for this theoretical approach, and are in very good agreement with experimental and numerical observations in supercooled liquids.

The physical picture which emerges from our work is, however, markedly different from that of the MCT/landscape scenario discussed in the Introduction.

At high temperatures, $T>T_o$, the dynamics is fast and liquidlike, corresponding to the relaxation of large clusters of defects. Dynamic facilitation plays no major role, and a simple mean-field Hartree-like decoupling of the equations of motion yields predictions in good agreement with numerical results.

When $T<T_o$, the dynamics becomes heterogeneous, in the sense that local relaxation times are spatially correlated in a nontrivial way. This can be seen in the trajectories of Fig. 2 as the appearance of slow bubbles [5,6]. The long-time dynamics of the system results from the wide joint distribution of length scales and time scales, and the relaxation becomes stretched. This dynamic heterogeneity, which can be thought of as the activated dynamics invoked, but never described, by MCT, determines the α relaxation and its temperature dependence for $T<T_o$. Also, dynamic heterogeneity implies that decoupling of transport coefficients actually starts at T_o, as confirmed by the simulations. From a theoretical point of view, local fluctuations of mobility crucially influence the dynamical behavior. Any mean-field-like approach, no matter how involved, is most probably doomed to fail.

At T_o not all trace of high-T physics (clusters of defects) disappears. The dynamics has a mixed character in the range $T_c<T<T_o$, as seen, for example, in the behavior of dynamical correlators like in Fig. 5. The temperature T_c is just a crossover. It is the temperature below which isolated defects not only dominate the long-time dynamics (as for $T_c<T<T_o$) but are also the most numerous dynamical objects, see Eq. (4). Clusters of defects, whose dynamics is homogeneous and nonactivated, are responsible for the temperature dependence of several quantities, such as distance between configurations and IS, saddle index $n_s(T)$, and anharmonic contributions to the free energy. In numerical simulations, T_c has been interpreted as a key temperature, in accordance with MCT for which it represents a dynamical singularity. We have shown, however, that all of these quantities have a smooth temperature dependence, as has been recently observed numerically [36–38]. This means that T_c does not correspond to a transition or singular point, but is at most a crossover. Crucially, the objects which display a crossover close to T_c are also irrelevant for the long-time dynamics, so that the inexistence of the singularity T_c is anyway not a physically important issue for the α relaxation.

Below T_c, isolated defects are the only remaining objects and the dynamics is dominated by the nanoscopic demixing of slow and fast regions so that trajectories look like a dense mixture of slow bubbles, which in turn gives a natural theoretical interpretation of the canonical features of glass transition phenomena [5–7].

Our results, together with some other recent studies [38,44,45,48,53,60,62–64,68], suggest that several essential features of the dynamics of supercooled liquids need to be recognized and we now list some of them.

(1) The dynamics is heterogeneous and activated well above T_c.

(2) The dynamical slowing down of supercooled liquids is due to the growth, below T_o, of a dynamic correlation length $\ell(T)$, or more precisely, of a whole distribution of length and time scales.

(3) The long-time dynamics, and therefore the relaxation time τ_α of the liquid is dominated by heterogeneous ''activated'' dynamics below T_o.

(4) The MCT definition of activated processes as deviations from the ideal theory is incorrect. It is unlikely that the power-law behavior predicted by MCT correctly describes the temperature dependence of τ_α. The practical definition of the temperature T_c cannot be used.

(5) No topological change of the potential energy landscape takes place close to T_c. Quantities such as the saddle index and anharmonicities do not vanish close to T_c and have a smooth temperature behavior. At best, they undergo a crossover from large to small which remains to be quantified.

(6) Even if one accepts T_c as a crossover temperature, as in Eq. (4), quantities related to this crossover are unimportant for the long-time dynamics.

(7) Knowledge of thermodynamic properties is not enough to predict dynamical behavior, which explains the quantitative failure of relations like the Adams-Gibbs formula.

The approach we developed in this paper, which is an extension of previous efforts [5–8], is generic. It can be applied both to systems like Lennard-Jones liquids or to hard sphere systems. It gives a perspective on the physics of glass formers which is clearly distinct to, and in many respects more natural than, that of MCT or topographic approaches.

There are many important and interesting open questions which need to be addressed from this perspective. This include, among others, understanding properly the origin of mobility excitations, and the breakdown of Stokes-Einstein-Debye relations and associated decouplings between transport coefficients.

A general conclusion that can be drawn from this work and our previous ones is that, in many respects, glass transition phenomenon is more standard than often assumed, in the sense that it is determined by the interplay between growing dynamic length scales and time scales. This is obviously reminiscent of critical phenomena [8], meaning that it should be possible to adapt renormalization group techniques to study the dynamics of the glass transition.

ACKNOWLEDGMENTS

We are grateful to J.-P. Bouchaud, G. Biroli, A. Buhot, A. Heuer, D.R. Reichman, G. Tarjus, and especially D. Chandler for useful discussions. We acknowledge financial support from CNRS (France), Marie Curie Grant No. HPMF-CT-2002-01927 (EU), EPSRC Grant No. GR/R83712/01, the Glasstone Fund, and Worcester College Oxford. Some of the numerical results were obtained on Oswell at the Oxford Supercomputing Center, Oxford University.

[1] M.D. Ediger, C.A. Angell, and S.R. Nagel, J. Phys. Chem. **100**, 13200 (1996).
[2] C.A. Angell, Science **267**, 1924 (1995).
[3] P.G. Debenedetti and F.H. Stillinger, Nature (London) **410**, 259 (2001).
[4] P. G. Debenedetti, *Metastable Liquids* (Princeton University Press, Princeton, 1996).
[5] J.P. Garrahan and D. Chandler, Phys. Rev. Lett. **89**, 035704 (2002).
[6] L. Berthier and J. P. Garrahan, J. Chem. Phys. **119**, 4367 (2003).
[7] J.P. Garrahan and D. Chandler, Proc. Natl. Acad. Sci. U.S.A. **100**, 9710 (2003).
[8] L. Berthier, Phys. Rev. Lett. **91**, 055701 (2003).
[9] W. Götze and L. Sjögren, Rep. Prog. Phys. **55**, 55 (1992).
[10] W. Götze, J. Phys.: Condens. Matter **11**, A1 (1999).
[11] W. Kob, in *Slow Relaxations and Nonequilibrium Dynamics in Condensed Matter*, edited by J.-L. Barrat, J. Dalibard, M.V. Feigel'man, and J. Kurchan, (Springer-Verlag, Berlin, 2003), cond-mat/0212344.
[12] For reviews on dynamic heterogeneity, see, H. Sillescu, J. Non-Cryst. Solids **243**, 81 (1999); M.D. Ediger, Annu. Rev. Phys. Chem. **51**, 99 (2000).
[13] W. Kob and H.C. Andersen, Phys. Rev. Lett. **73**, 1376 (1994); Phys. Rev. E **51**, 4626 (1995); **52**, 4134 (1995).
[14] W. Götze and T. Voigtmann, Phys. Rev. E **61**, 4133 (2000).
[15] G. Tarjus and D. Kivelson, in *Jamming and Rheology*, edited by A. J. Liu and S. R. Nagel (Taylor & Francis, New York, 2001).
[16] E. J. Donth, *The Glass Transition* (Springer-Verlag, Berlin, 2001).
[17] E. Rössler and A.P. Sokolov, Chem. Geol. **128**, 143 (1996).
[18] F. Stickel, E.W. Fischer, and R. Richert, J. Chem. Phys. **104**, 2043 (1996).
[19] C.A. Angell, J. Phys. Chem. Solids **49**, 863 (1988); J. Phys.: Condens. Matter **12**, 6463 (2000).
[20] M. Goldstein, J. Chem. Phys. **51**, 3728 (1969).
[21] F.H. Stillinger and T.A. Weber, Phys. Rev. A **25**, 978 (1982); **28**, 2408 (1983); Science **225**, 983 (1984).
[22] F.H. Stillinger, Science **267**, 1935 (1995).
[23] S. Sastry, P.G. Debenedetti, and F.H. Stillinger, Nature (London) **393**, 554 (1998).
[24] S. Büchner and A. Heuer, Phys. Rev. E **60**, 6518 (1999).
[25] S. Büchner and A. Heuer, Phys. Rev. Lett. **84**, 2168 (2000).
[26] T.B. Schroder, S. Sastry, J.C. Dyre, and S.C. Glotzer, J. Chem. Phys. **112**, 9834 (2000).
[27] P. Jund and R. Jullien, Phys. Rev. Lett. **83**, 2210 (1999).
[28] T. Keyes and J. Chowdhary, Phys. Rev. E **65**, 041106 (2002).
[29] For extension of the landscape ideas in the glass phase see: C.A. Angell, Y. Yue, L.M. Wang, J.R.D. Copley, S. Borick, and S. Mossa, J. Phys. C **15**, S1051 (2003); T.S. Grigera, V. Martin-Mayor, G. Parisi, and P. Verrocchio, Nature (London) **422**, 289 (2003); for alternative real space interpretations, see, e.g., E. Duval, L. Saviot, L. David, S. Etienne, and J. F. Jal, Europhys. Lett. **63**, 778 (2003).
[30] A. Cavagna, Europhys. Lett. **53**, 490 (2001).
[31] J. Kurchan and L. Laloux, J. Phys. A **29**, 1929 (1996).
[32] A. Cavagna, J.P. Garrahan, and I. Giardina, Phys. Rev. B **61**, 3960 (2000).
[33] K. Broderix, K.K. Bhattacharya, A. Cavagna, A. Zippelius, and I. Giardina, Phys. Rev. Lett. **85**, 5360 (2000).
[34] L. Angelani, R. Di Leonardo, G. Ruocco, A. Scala, and F. Sciortino, Phys. Rev. Lett. **85**, 5356 (2000).
[35] P. Shah and C. Chakravarty, J. Chem. Phys. **115**, 8784 (2001); T.S. Grigera, A. Cavagna, I. Giardina, and G. Parisi, Phys. Rev. Lett. **88**, 055502 (2002); L. Angelani, R. Di Leonardo, G. Ruocco, A. Scala, and F. Sciortino, J. Chem. Phys. **116**, 10297 (2002); L. Angelani, G. Ruocco, M. Sampoli, and F. Sciortino, J. Chem. Phys. **119**, 2120 (2003).
[36] J.P.K. Doye and D.J. Wales, J. Chem. Phys. **116**, 3777 (2002).
[37] G. Fabricius and D.A. Stariolo, Phys. Rev. E **66**, 031501 (2002).
[38] B. Doliwa and A. Heuer, Phys. Rev. E **67**, 031506 (2003).
[39] A. Cavagna, I. Giardina, and G. Parisi, J. Phys. A **34**, 5317 (2001).
[40] S.D. Bembenek and B.B. Laird, Phys. Rev. Lett. **74**, 936 (1995); J. Chem. Phys. **104**, 5199 (1996).
[41] C. Donati, F. Sciortino, and P. Tartaglia, Phys. Rev. Lett. **85**, 1464 (2000); E. La Nave, H.E. Stanley, and F. Sciortino, *ibid.* **88**, 035501 (2002).
[42] T. Keyes, J. Phys. Chem. **101**, 2921 (1997).
[43] W. Kob, J.-L. Barrat, F. Sciortino, and P. Tartaglia, J. Phys. C **12**, 6385 (2000).
[44] B. Doliwa and A. Heuer, Phys. Rev. E **67**, 030501 (2003).
[45] R.A. Denny, D.R. Reichman, and J.-P. Bouchaud, Phys. Rev. Lett. **90**, 025503 (2003).
[46] See for a review, S.C. Glotzer, J. Non-Cryst. Solids **274**, 342 (2000).
[47] G. Tarjus and D. Kivelson, J. Chem. Phys. **103**, 3071 (1995).
[48] P. Viot, G. Tarjus, and D. Kivelson, J. Chem. Phys. **112**, 10 368 (2000); D.N. Perera and P. Harrowell, Phys. Rev. E **54**, 1652 (1996).
[49] S.H. Glarum, J. Chem. Phys. **33**, 639 (1960); M.C. Phillips, A.J. Barlow, and J. Lamb, Proc. R. Soc. London, Ser. A **329**, 193 (1972).
[50] P. W. Anderson, in *Ill-Condensed Matter*, edited by R. Balian *et al.* (North-Holland, Amsterdam, 1979).
[51] R. G Palmer, D.L. Stein, E. Abrahams, and P.W. Anderson, Phys. Rev. Lett. **53**, 958 (1984).
[52] G.H. Fredrickson and H.C. Andersen, Phys. Rev. Lett. **53**,

1244 (1984); J. Chem. Phys. **83**, 5822 (1985).
[53] S. Butler and P. Harrowell, J. Chem. Phys. **95**, 4454 (1991); **95**, 4466 (1991); P. Harrowell, Phys. Rev. E **48**, 4359 (1993); M. Foley and P. Harrowell, J. Chem. Phys. **98**, 5069 (1993).
[54] F. Ritort and P. Sollich, Adv. Phys. **52**, 219 (2003).
[55] J.P. Garrahan and M.E.J. Newman, Phys. Rev. E **62**, 7670 (2000); J.P. Garrahan, J. Phys. C **14**, 1571 (2002).
[56] S. Franz, C. Donati, G. Parisi, and S.C. Glotzer, Philos. Mag. B **79**, 1827 (1999); S.C. Glotzer, V. Novikov, and T.B. Schroder, J. Chem. Phys. **112**, 509 (2000).
[57] B. Doliwa and A. Heuer, Phys. Rev. E **61**, 6898 (2000).
[58] M.M. Hurley and P. Harrowell, Phys. Rev. E **52**, 1694 (1995); D.N. Perera and P. Harrowell, J. Chem. Phys. **111**, 5441 (1999).
[59] Y. Hiwatari and T. Muranaka, J. Non-Cryst. Solids **235-237**, 19 (1998).
[60] B. Doliwa and A. Heuer, e-print cond-mat/0306343.
[61] M. Schulz and S. Trimper, Phys. Rev. E **57**, 6398 (1998).
[62] X.C. Zeng, D. Kivelson, and G. Tarjus, Phys. Rev. E **50**, 1711 (1994).
[63] X.C. Zeng, D. Kivelson, and G. Tarjus, Phys. Rev. Lett. **72**, 1772 (1994).
[64] Y. Brumer and D.R. Reichman, e-print cond-mat/0306580.
[65] A. Crisanti, F. Ritort, A. Rocco, and M. Sellitto, J. Chem. Phys. **113**, 10 615 (2000).
[66] D. Kivelson and G. Tarjus, J. Phys. Chem. B **105**, 11854 (2001).
[67] F.H. Stillinger, J. Chem. Phys. **88**, 7818 (1988).
[68] D. Kivelson, S.A. Kivelson, X. Zhao, Z. Nussinov, and G. Tarjus, Physica A **219**, 27 (1995).